ELSEVIER

Biophysical Chemistry 72 (1998) 285–295

Biophysical Chemistry

Computer simulation of damped oscillations during peroxidase-catalyzed oxidation of indole-3-acetic acid

Sergey N. Krylov *

Department of Chemistry, University of Alberta, Edmonton, Alberta, Canada T6G 2G2

Received 20 November 1997; revised 23 January 1998; accepted 23 January 1998

Abstract

Oscillation patterns in horseradish peroxidase (HRP)-catalyzed oxidation of indole-3-acetic acid (IAA) at neutral pH were studied using computer simulation. Under certain conditions, such as the presence of a reaction promoter and continuous intake of oxygen from the gaseous phase, the simulated system exhibits damped oscillations of the concentrations of oxygen in the aqueous phase, $[O_2]^{aq}$, and of all the reaction intermediates. The critical concentration of oxygen in aqueous phase, $[O_2]^{aq}_{cr}$, was used to describe the nature of the oscillations. The critical concentration is the concentration at which the system abruptly changes its properties. If $[O_2]^{aq}$ is higher than $[O_2]^{aq}_{cr}$ then the reaction develops as an avalanche, otherwise, the reaction stops. The nature of oscillations is accounted for by the interaction of two processes: the consumption/accumulation of oxygen and the accumulation/consumption of reaction intermediates. Oscillations are always damped. Neither HRP or umbelliferone (Umb) deactivation nor IAA consumption can account for the damping. The nature of the damping is determined by the termination reactions of free radical intermediates and ROOH. The three major parameters of oscillations: period of oscillations, initial amplitude of oscillations and the rate of damping were studied as functions of: (i) oxygen concentration in the gaseous phase, (ii) initial oxygen concentration in aqueous phase, (iii) the concentration of IAA and (iv) the initial concentration of HRP.

Keywords: Horseradish peroxidase; Indole-3-acetic acid oxidation; Damped oscillations; Modelling; Computer simulation

1. Introduction

Peroxidases are able to catalyze the oxidation of several substrates aerobically without added peroxide. Among these substrates are: indole-3-acetic acid (IAA) [1–9], NADH [10,11], dihydroxyfumarate [12], and isobutyraldehyde [13]. These peroxidase-catalyzed O_2-consuming processes are called peroxidase–oxidase reactions. Peroxidase–oxidase reactions are of interest to researchers because: (i) they exhibit a number of non-linear dynamic behaviors such as bistabilities, oscillations, and chaos [7,10,11,14–19]; (ii) they produce chemiluminescence [13,20–22]; and (iii) at least one of them (oxidation of IAA) is an important physiological reaction [23]. IAA is a phytohormone with many growth regulatory functions [24]. The peroxidase-catalyzed oxidation of IAA plays an important role in IAA catabolism in vivo and thus in control of plant growth [25].

IAA oxidation by horseradish peroxidase (HRP) is a very complex process in which many reaction

* Corresponding author. Tel.: +1-403-492-9251; fax: +1-403-492-8231; e-mail: sergey.krylov@ualberta.ca

0301-4622/98/$19.00
PII S0301-4622(98)00109-4

intermediates and final products are formed [26]. Moreover, during the course of the reaction, HRP is converted from the native enzyme into several catalytic and inactive forms [5,27,28]. Two main reaction pathways for the HRP-catalyzed oxidation of IAA have been recognized, labelled peroxidase pathway and oxidase pathway. In the classical peroxidase pathway, hydroperoxide (ROOH) is the two-electron oxidizing substrate of the native enzyme, converting it into compound I. IAA is the one-electron reducing substrate for both of the enzyme intermediates, compound I (HRP-I) and compound II (HRP-II). A non-classical part of the peroxidase pathway is a free radical chain reaction in which ROOH is regenerated [2,5–9]. The oxidase pathway involves the ferrous enzyme (Fe^{2+}-HRP) and compound III (HRP-III) [3]. The substrate of Fe^{2+}-HRP is oxygen and the substrate of HRP-III is IAA [3,4]. The pathway which is followed depends upon the experimental conditions. A high pH promotes the peroxidase pathway while a low pH favors the oxidase pathway [3–5]. In a recent paper Gazaryan et al. [29] suggested a relatively simple alternative mechanism for the HRP-catalyzed IAA oxidation. They postulated that a ternary complex of native ferric HRP, IAA and O_2 plays a key role in both the initiation step and subsequent reaction cycle. However, this hypothesis is speculative, since no evidence for the ternary complex was presented.

The mechanism of HRP-catalyzed IAA oxidation at neutral pH has been intensively studied for the last 2 years [5–9]. It was shown that IAA is oxidized by a combination of both an enzymatic cycle and a free radical chain reaction [5]. The enzymatic cycle produces free radicals of IAA required for sustaining a free radical chain, while a free radical chain reaction produces ROOH needed for sustaining the enzymatic cycle. It was shown that the symbiotic effect of the enzymatic cycle and the free radical chain reaction is so efficient that no additional steps are required for initiating the reaction; the traces of ROOH derived from IAA, which cannot be totally eliminated from the IAA solutions, are all that is required for the initiation [6,7]. Phenols are known to be either inhibitors or promoters of HRP-catalyzed IAA oxidation [30]. The mechanisms of the phenol-induced inhibition and acceleration of the HRP-catalyzed IAA oxidation were studied using caffeic acid [7], and umbelliferone (Umb) [9], as an inhibitor and a promoter, respectively. Caffeic acid acts mainly as a competitive substrate of HRP-I and HRP-II. The free radical scavenging ability of caffeic acid can also contribute to the inhibition but only at relatively high concentrations. Umb-induced enhancement of the HRP-catalyzed IAA oxidation is ascribed to a combination of three accelerating effects: (i) the reduction of the rate-limiting HRP species, HRP-II, by Umb, which increases the rate of enzymatic IAA oxidation, (ii) non-enzymatic oxidation of IAA by free radicals of Umb formed in the HRP-catalyzed oxidation of Umb and (iii) Umb-induced acceleration of HRP-I reduction by IAA. A detailed model of the HRP-catalyzed IAA oxidation has been developed [6,9], and applied to the analysis of phenol-induced inhibition [7].

Oscillations in the peroxidase–oxidase reactions were observed for the first time by Yamazaki [14] using NADH as a substrate of HRP. The $NADH/HRP/O_2$ system has been studied very intensively since then (see Ref. [15] for review). Nonlinear behaviors in HRP-catalyzed IAA oxidation were also studied although not as much as in the $NADH/HRP/O_2$ system. Degn [16] observed damped oscillations during HRP-catalyzed IAA oxidation in his earlier work. After this work there were no further publications concerning oscillations in the $IAA/HRP/O_2$ system. The lack of experimental efforts in studying the $IAA/HRP/O_2$ oscillator was, in particular, due to the absence of a detailed model of HRP-catalyzed IAA oxidation.

This paper presents the first computer simulation of the oscillation patterns in the $IAA/HRP/O_2$ system using the detailed mechanism of HRP-catalyzed IAA oxidation at neutral pH. It was found that the simulated system exhibits damped oscillations, similar to those observed by Degn in his earlier experiments, under continuous oxygen intake and in the presence of a cofactor.

2. Procedures

A Pentium computer operating at 120 MHz was used for the computer simulations. A program for integration of reaction rate equations was written in Fortran and compiled with Microsoft Fortran Power-

Station. The program used a Runge–Kutta procedure with adaptive step size control [31], and operated in double precision mode. Output data were the simulated concentrations of all the reaction species as functions of time for 100 min. The data were processed and analyzed in an Excel spreadsheet. Except where otherwise noted, the rate constant values were those given in Table 1, while differential equations and initial concentrations were those listed in Table 2.

The maxima of oscillating concentrations $C^{max}(t)$ were determined using the following algorithm:

$$C(t) \equiv C^{max}(t) \text{ if } C(t) \geq C(t - i\Delta t) \text{ and } C(t) > C(t + i\Delta t) \quad (1)$$

where $C(t)$ is the concentration at time t, Δt is the time interval equal to 0.1 min and $i = 1,2,3,4,5$.

In order to determine the first-order rate constant k for the damping of oscillations the data for the maxima were fit by single-exponential function with floating endpoint:

$$C^{max}(t) = C^{max}(t_\infty) + (C^{max}(t_0) - C^{max}(t_\infty))e^{-k(t-t_0)} \quad (2)$$

where t_0 is time of the first maximum and t_∞ is an infinity time; $C^{max}(t_\infty)$ and k were variables, whereas $C^{max}(t)$ was determined in a computer experiment. Fitting procedure was performed using Origin software.

3. Reaction model

The reaction scheme presented in Fig. 1 describes the mechanism of HRP-catalyzed oxidation of IAA in the presence of a cofactor, Umb [9]. All the reactions involved in the mechanism are listed in Table 1 together with the corresponding rate constants. Reaction 1 is a very slow non-enzymatic process, responsible for the production of traces of

Table 1
Main reactions involved in the HRP-catalyzed oxidation of IAA at pH 7.4 in the presence of Umb and oxygen intake from gaseous phase to the reaction mixture

No.	Reaction	Rate constants	Refs.
1	$IAA \rightarrow IAA^{+\cdot}$	$k_1 = 3 \times 10^{-7}\ s^{-1}$	[7]
2	$IAA^{+\cdot} \rightarrow R^{\cdot} + CO_2$	$k_2 = 90\ s^{-1}$	[32]
3	$R^{\cdot} + O_2 \rightarrow ROO^{\cdot}$	$k_3 = 2.0 \times 10^8\ M^{-1}\ s^{-1}$	[32]
4	$ROO^{\cdot} + IAA \rightarrow ROOH + IAA^{+\cdot}$	$k_4 = 1.0 \times 10^6\ M^{-1}\ s^{-1}$	[6]
5	$IAA^{+\cdot} + IAA^{+\cdot} \rightarrow P_1$	$2k_5 = 5.3 \times 10^8\ M^{-1}\ s^{-1}$	[32]
6	$R^{\cdot} \rightarrow P_2$	$k_6 = 1.8 \times 10^4\ s^{-1}$	[6]
7	$ROO^{\cdot} \rightarrow P_3$	$k_7 = 5.62\ s^{-1}$	[6]
8	$ROOH \rightarrow P_4$	$k_8 = 1.45 \times 10^{-3}\ s^{-1}$	[2,6]
9	$HRP + ROOH \rightarrow HRP\text{-}I + ROH$	$k_9 = 2.0 \times 10^6\ M^{-1}\ s^{-1}$	[2,6]
10	$HRP\text{-}I + IAA \rightarrow HRP\text{-}II + IAA^{+\cdot}$	$k_{10} = 2.3 \times 10^3\ M^{-1}\ s^{-1}$	[5,6]
10′[a]	$HRP\text{-}I + IAA \xrightarrow{UMB} HRP\text{-}II + IAA^{+\cdot}$	$k'_{10} = 2.3 \times 10^4\ M^{-1}\ s^{-1}$	[9]
11	$HRP\text{-}II + IAA \rightarrow HRP + IAA^{+\cdot}$	$k_{11} = 2.05 \times 10^2\ M^{-1}\ s^{-1}$	[5,6]
12	$HRP\text{-}II \rightarrow HRP$	$k_{12} = 1.75 \times 10^{-3}\ s^{-1}$	[6]
13	$HRP\text{-}I + ROOH \rightarrow P\text{-}670$	$k_{13} = 6.2 \times 10^2\ M^{-1}\ s^{-1}$	[6]
14	$HRP\text{-}I + Umb \rightarrow HRP\text{-}II + Umb^{\cdot}$	$k_{14} = 1.1 \times 10^5\ M^{-1}\ s^{-1}$	[9]
15	$HRP\text{-}II + Umb \rightarrow HRP + Umb^{\cdot}$	$k_{15} = 1.7 \times 10^5\ M^{-1}\ s^{-1}$	[9]
16	$Umb^{\cdot} + IAA \rightarrow Umb + IAA^{+\cdot}$	$k_{16} = 1 \times 10^6\ M^{-1}\ s^{-1}$	[b]
17	$Umb^{\cdot} + Umb^{\cdot} \rightarrow P_5$	$k_{17} = 1 \times 10^8\ M^{-1}\ s^{-1}$	[b]
18	$O_2^{gas} \rightarrow O_2^{aq}$	$k_{18} = 1 \times 10^{-6}\ s^{-1}$	[b]
19	$O_2^{aq} \rightarrow O_2^{gas}$	$k_{19} = K_{eq} \times k_{18}$[c]	[10]

[a] The rate of Reaction 10 increases by a factor of 10 in the presence of 1 μM Umb.
[b] Present paper.
[c] $K_{eq} = 34.25$.

Table 2
Rate equations[a] and parameters used for computer simulation of damped oscillations during the HRP-catalyzed IAA oxidation

Rate equations

(1) $d[IAA]/dt = 0$

(2) $d[IAA^{+\cdot}]/dt = (k_1 + k_4\,[ROO^{\cdot}] + k_{10}[HRP\text{-}I] + k_{11}[HRP\text{-}II] + k_{16}[Umb])\,[IAA] - (k_2 + 2k_5[IAA^{+\cdot}])[IAA^{+\cdot}]$

(3) $d[R^{\cdot}]/dt = k_2[IAA^{+\cdot}] - (k_3[O_2]^{aq} + k_6)[R^{\cdot}]$

(4) $d[O_2]^{aq}/dt = -k_3[O_2]^{aq}[R^{\cdot}] + k_{18}([O_2]^{gas} - K_{eq}[O_2]^{aq})$

(5) $d[O_2]^{gas}/dt = 0$

(6) $d[ROO^{\cdot}]/dt = k_3[O_2]^{aq}[R^{\cdot}] - (k_4\,[IAA] + k_7)\,[ROO^{\cdot}]$

(7) $d[ROOH]/dt = k_4[ROO^{\cdot}][IAA] - (k_8 + k_9[HRP] + k_{13}[HRP\text{-}I])[ROOH]$

(8) $d[HRP]/dt = (k_{11}[IAA] + k_{12})[HRP\text{-}II] - k_9[HRP][ROOH]$

(9) $d[HRP\text{-}I]/dt = k_9[HRP][ROOH] - (k_{10}[IAA] + k_{13}[ROOH] + k_{14}[Umb])[HRP\text{-}I]$

(10) $d[HRP\text{-}II]/dt = k_{10}[HRP\text{-}I][IAA] - (k_{11}[IAA] + k_{12} + k_{15}[Umb])[HRP\text{-}II]$

(11) $d[P\text{-}670]/dt = k_{13}[HRP\text{-}I][ROOH]$

(12) $d[Umb]/dt = -(k_{14}[HRP\text{-}I] + k_{15}[HRP\text{-}II])[Umb] + k_{16}[IAA][Umb^{\cdot}]$

(13) $d[Umb^{\cdot}]/dt = (k_{14}[HRP\text{-}I] + k_{15}[HRP\text{-}II])[Umb] - k_{16}[IAA]\,[Umb^{\cdot}] - 2k_{17}[Umb^{\cdot}]^2$

Initial concentrations

$[HRP]_0 = 1\ \mu M$

$[IAA]_0 = 100\ \mu M$ = constant

$[O_2]_0^{aq} = 100\ \mu M$

$[ROOH]_0 = 2.7 \times 10^{-4}[IAA]_0$ (Ref. [7])

All other initial concentrations are zero

Integration parameters

stepsize lower limit = 0

stepsize error = 1×10^{-2}

[a] The rate constant k'_{10} was used instead of k_{10} for non-zero concentrations of Umb.

$IAA^{+\cdot}$ (cation radical of IAA) in the absence of HRP [7]. This reaction is important for the initiation of enzymatic oxidation (particularly in the presence of inhibitors), but does not play any significant role during the steady state HRP-catalyzed IAA oxidation [7]. $IAA^{+\cdot}$ tends to deprotonate rapidly at neutral pH; however, there is an equilibrium fraction of protonated $IAA^{+\cdot}$ which can decarboxylate to the skatolyl radical $R^{\cdot}$ (Reaction 2) [7]. $R^{\cdot}$, in turn, is rapidly scavenged by O_2 to form indole-3-methyl hydroperoxyl radical, $ROO^{\cdot}$ (Reaction 3) [32,33]. $ROO^{\cdot}$ reacts with IAA producing $IAA^{+\cdot}$ and indole-3-methyl hydroperoxide, ROOH (Reaction 4). Reactions 5–8 are termination steps for the intermediates $IAA^{+\cdot}$, $R^{\cdot}$, $ROO^{\cdot}$ and ROOH [6]. It was shown that $IAA^{+\cdot}$ undergoes bimolecular radical–radical recombination (Reaction 5) [32], whereas the termination steps for $R^{\cdot}$ and $ROO^{\cdot}$ and ROOH are satisfactorily described by unimolecular Reactions 6–8 [6]. The reaction sequence 1–8 is a complex free radical chain process, producing two essential intermediates: $IAA^{+\cdot}$ and ROOH. These reactions are responsible for the presence of traces of ROOH in the IAA solution in the absence of HRP [7]; after HRP addition, these traces of ROOH initiate HRP participation in the reaction. During the steady state the reaction sequence 1–8 regenerates ROOH required for sustaining the enzymatic cycle.

IAA is oxidized in the standard peroxidase cycle (Reactions 9–11). Two cation radicals required for sustaining the free radical chain are produced during one HRP turnover. HRP-II is slowly reduced in the absence of IAA (Reaction 12) [5,6]. Reaction 13 represents a rate-limiting step in the formation of inactive verdohemoprotein, P-670 [5,6]. The essence of the mechanism is that a trace of peroxide (ROOH) is all that is required to initiate the reaction. The combination of the non-enzymatic free radical chain and the peroxidase cycle continually produces ample ROOH for the reaction to reach and maintain its maximal steady state rate, which is maintained until inactivation processes become dominant.

The presence of Umb results in acceleration of IAA oxidation due to three effects: (i) the reduction

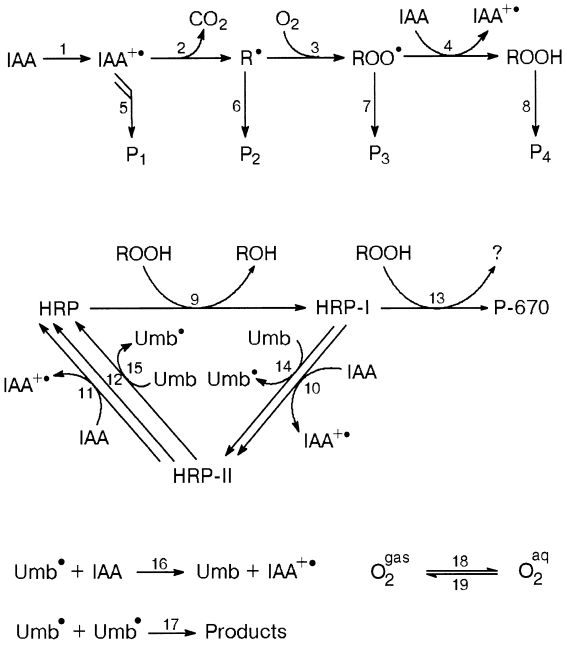

Fig. 1. Detailed mechanism of HRP-catalyzed oxidation of IAA in the presence of a cofactor, Umb.

of HRP-II by Umb, (ii) oxidation of IAA by free radicals of Umb and (iii) Umb-induced acceleration of HRP-I reduction by IAA [9]. Therefore, Reactions 14–17 were included in the mechanism of IAA oxidation in the presence of Umb. Reactions 14 and 15 are oxidation reactions of Umb by HRP-I and HRP-II, respectively. Reaction 16 is the oxidation of IAA by the free radical of Umb ($Umb^{\cdot}$). Reaction 17 represents recombination of free radicals of Umb. Umb-induced enhancement of HRP-I reduction by IAA is represented by 10-fold increase in corresponding rate constant (compare k_{10} and k'_{10} in Table 1).

Our model system is open for gas diffusion. Therefore, oxygen can freely diffuse from the gaseous phase to the reaction mixture (Reaction 18) and from the reaction mixture to the gaseous phase (Reaction 19). The concentration of oxygen in the gaseous phase is represented as $[O_2]^{gas}$ and that in the aqueous phase as $[O_2]^{aq}$.

All the rate constants used in the present study are listed in Table 1. Rate constants k_1–k_{15} where obtained from the works of other authors and/or from our previous studies. Rate constant k_{16} was set at 1×10^6 M^{-1} s^{-1} to describe the experimentally observed 8-fold acceleration of HRP-catalyzed IAA oxidation in the presence of 1 μM Umb [9]. The rate constant $k_{17} = 1 \times 10^8$ M^{-1} s^{-1} is typical for radical–radical recombination and is in good agreement with a rough estimate of this rate constant, based on the results of Segawa et al. [34]. Rate constant k_{18} can be changed by varying the ratio between the volume of the reaction mixture and the area of the liquid–gas boundary. It was chosen to be 1×10^{-6} s^{-1} for the purpose of the present research (see rationale in Section 5.2). Rate constant k_{19} is determined by oxygen equilibrium between the aqueous and gaseous phases. Differential rate equations and parameters used in the computer simulation are listed in Table 2.

4. Critical concentration of oxygen

The overall reaction of HRP-catalyzed IAA oxidation exhibits all the properties of a free-radical chain process [5]. The reaction has two steady states: a 'low reaction rate' steady state and a 'high reaction rate' steady state [19,35]. Therefore, the critical values of the major reaction parameters, $[O_2]$, [IAA] and [HRP], at which the reaction switches from one steady state to the other, should exist. In theoretical studies of chemical bistabilities the critical concentrations are often called 'unstable fixed point in the system with three fixed points: two stable and one unstable'. A typical design of oscillation experiment in this peroxidase–oxidase system involves a quasi-constant concentration of the substrate and intake of O_2 from the gaseous phase to the aqueous phase. In the present computer simulations similar conditions were used: constant [IAA] and free intake of O_2 from the gaseous phase to the reaction mixture. In such a design the critical concentration of oxygen in the aqueous phase, $[O_2]^{aq}_{cr}$, has a crucial role, since the oscillations of $[O_2]^{aq}$ appear virtually around $[O_2]^{aq}_{cr}$ (see Section 5.4). $[O_2]^{aq}_{cr}$ was determined as a function of [HRP] and [IAA]. It was found that $[O_2]^{aq}_{cr}$ does not depend on [HRP] varied within the range of 10^{-7}–10^{-5} M (data not shown; $[O_2]^{aq}_{cr}$ was determined within 1% accuracy at fixed IAA concentration of 10^{-5} M). $[O_2]^{aq}_{cr}$ decreases with increasing [IAA] (Fig. 2). The presence of Umb results in

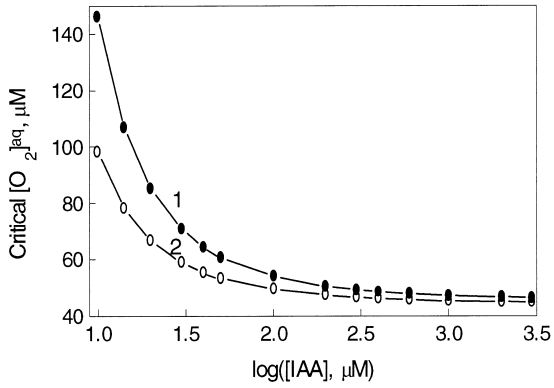

Fig. 2. The effect of IAA concentration on the critical concentration of O_2 in the aqueous phase. Simulated system contained 1 μM HRP and either no Umb (1) or 1 μM Umb (2).

decreasing $[O_2]^{aq}_{cr}$ (Fig. 2, curve 2). It should be noted that the data $[O_2]^{aq}_{cr}$ vs. [IAA] (Fig. 2) can be also represented as $[IAA]_{cr}$ vs. $[O_2]^{aq}$ since the critical parameters are interrelated.

5. Damped oscillations

5.1. The nature of the oscillations

Almost ninety years ago Lotka showed that autocatalytic reactions in an open system exhibit damped oscillations for certain values of the reaction parameters [36]. Damped oscillations were found experimentally in the peroxidase–oxidase reaction for three substrates: NADH, dihydroxyfumaric acid and IAA [10,11,14–18]. The applicability of Lotka's theory to peroxidase–oxidase reactions was later confirmed theoretically using the simplified model of peroxidase–oxidase system [17].

Here, the detailed model of the HRP-catalyzed IAA oxidation in the presence of a cofactor, Umb [9], and under permanent oxygen intake, is studied. It was found that under certain values for oxygen intake parameters the system exhibits damped oscillations. Fig. 3 shows an example of oscillations for O_2, HRP species and all the reaction intermediates.

The nature of the oscillations involves the interaction of two processes: (i) oxygen consumption during HRP-catalyzed IAA oxidation and oxygen intake from the gaseous phase and (ii) intermediate accumulation during O_2-consuming phase and intermediate consumption after reaction stops. A good physical analogy is a pendulum. The difference between $[O_2]^{aq}_0$ and $[O_2]^{aq}_{cr}$ is the equivalent of potential energy, while the concentration of accumulating intermediates ($IAA^{+\cdot}$, $R^{\cdot}$, $ROO^{\cdot}$, ROOH, HRP-I and HRP-II) is the analog of kinetic energy. Let us assume that $[O_2]^{aq}_0 > [O_2]^{aq}_{cr}$, and $[O_2]^{gas} > K_{eq}[O_2]^{aq}_{cr}$. The second assumption just ensures that equilibrium $[O_2]^{aq}$ is higher than $[O_2]^{aq}_{cr}$, otherwise oscillations cannot exist. The mechanism of oscillations could be described in the following way. During the reaction $[O_2]^{aq}$ decreases while the concentration of intermediates increases. If there are no intermediates present, the reaction would stop when $[O_2]^{aq}$ reaches $[O_2]^{aq}_{cr}$. However, the intermediates accumulating in the reaction mixture drive oxygen consumption for a while even though $[O_2]^{aq} < [O_2]^{aq}_{cr}$. This results in a further decrease of $[O_2]^{aq}$. Oxygen consumption stops when all the intermediates are utilized at $[O_2]^{aq} < [O_2]^{aq}_{cr}$. O_2 then accumulates due to O_2 intake from the gaseous phase. The HRP-catalyzed IAA oxidation starts when $[O_2]^{aq} = [O_2]^{aq}_{cr}$. However, because of a reaction lag period caused by the lack of reaction intermediates the oxygen consumption in the system is negligible in the beginning [6,7]. Therefore, oxygen continues to accumulate for a certain time until the rate of its consumption exceeds the rate of its intake. The time when $[O_2]^{aq}$ reaches a maximum corresponds to the end of the first cycle and the start of the second cycle in oscillations. This process repeats once then over and over again until oscillations are completely damped.

The oscillations in the IAA/HRP/O_2 system are always damped. Neither HRP or Umb deactivation nor IAA consumption can account for damping. Indeed, assuming that [IAA] = constant and the rate constants of HRP and Umb deactivation, k_{13} and k_{17}, are zero does not sustain the oscillations. The nature of damping is in the termination reactions for free radical intermediates and ROOH. Decreasing the corresponding rate constants, k_5–k_8, results to decreasing rate of damping (not shown).

5.2. Oxygen transport

The rate of oxygen transport between the gaseous and aqueous phases is described by the equation

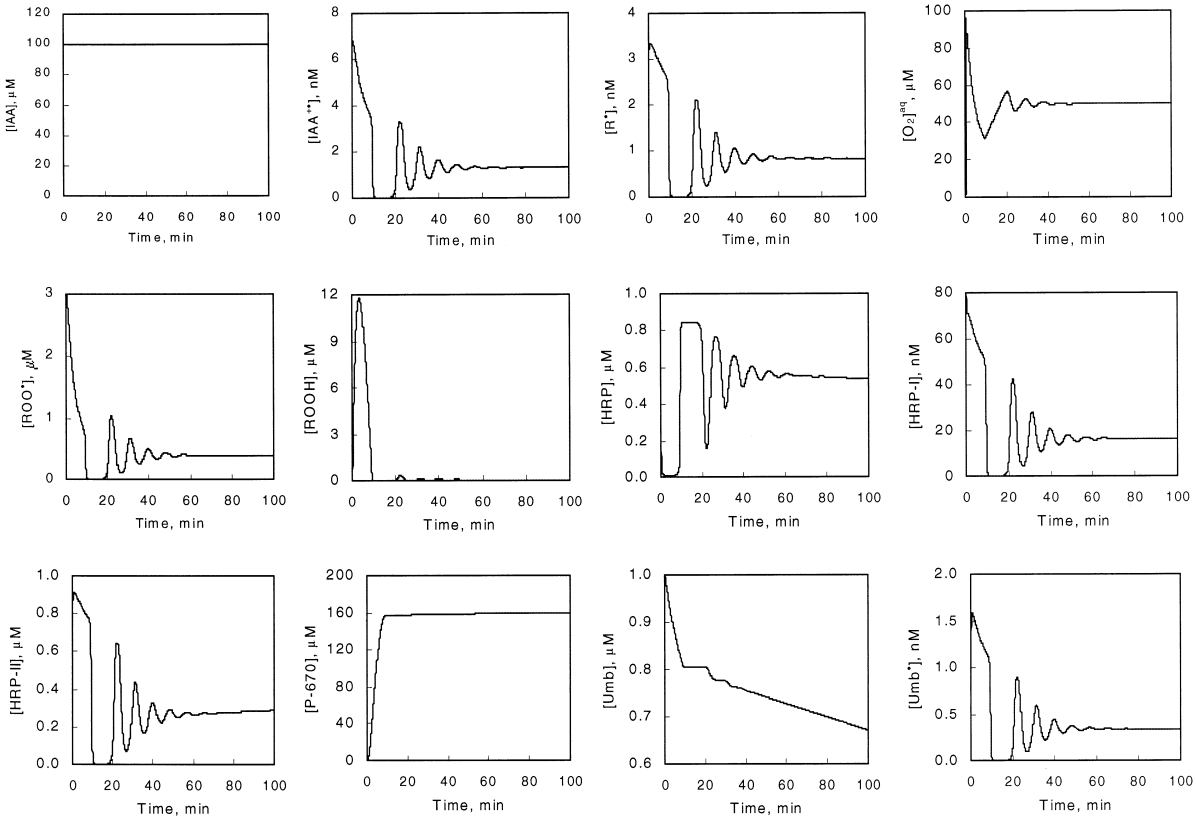

Fig. 3. Damped oscillations during HRP-catalyzed oxidation of IAA in the presence of Umb. The following parameters were used for simulations: $k_{18} = 1 \times 10^{-6}$ s^{-1}, $[O_2]_0^{aq} = 100$ μM, $[O_2]^{gas} = 43$ mM (partial pressure 14.2 psi), $[HRP]_0 = 1$ μM, [IAA] = 100 μM = constant and $[Umb]_0 = 1$ μM.

$d[O_2]^{aq}/dt = k_{18}([O_2]^{gas} - K_{eq}[O_2]^{aq})$ where k_{18} is the rate constant of oxygen diffusion from the gaseous phase to the aqueous phase and $K_{eq} = 34.25$ is the equilibrium constant for the exchange of oxygen between the gaseous and aqueous phases [10]. Oscillations are very sensitive to the parameters of O_2 transport. Fig. 4 shows the range of the parameters k_{18} and $[O_2]^{gas}$ in which oscillations exist (it is assumed here that oscillations do not exist if two maxima are not found in $[O_2]^{gas}$ kinetics). The lower limit of $[O_2]^{gas}$ (1.7 mM) is the concentration of $[O_2]^{gas}$ for which the corresponding equilibrium $[O_2]^{aq}$ is equal to $[O_2]_{cr}^{aq}$ (49.4 μM for the conditions used). The upper limit and, thus, the range of $[O_2]^{gas}$, for which oscillations exist, decrease considerably with increasing k_{18}. Therefore, it was unpractical to use $k_{18} = 10^{-4}$ s^{-1} which is usually employed in the experimental studies of the NADH/HRP/O_2 system [10–18]. For further investigation k_{18} was set at 10^{-6} s^{-1}. It should be noted that k_{18} can be easily changed in experiment by changing the ratio between the volume of the reaction mixture and the area of the surface separating the aqueous and gaseous phases under vigorous stirring of the solution.

5.3. Period of oscillations

The period of oscillations was estimated as the average of time intervals between $[O_2]^{aq}$ maxima for the reaction time of 100 min. These time intervals are not equal. However, there is no clear pattern in their changing. Therefore, those changes were simply represented as error bars for the values of the oscillation period. Initially, it was suspected that the source of error in the determination of the period of

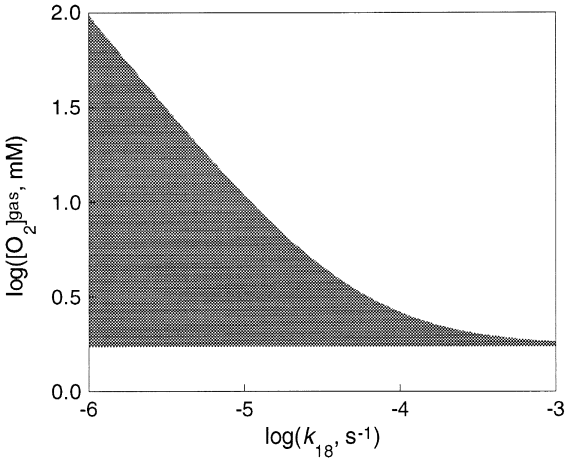

Fig. 4. Phase space of the parameters k_{18} and $[O_2]^{gas}$ in which the system exhibits the oscillations. The following parameters were used for simulations: $[O_2]_0^{aq} = 100\ \mu M$, $[HRP]_0 = 1\ \mu M$, $[IAA] = 100\ \mu M$ = constant and $[Umb]_0 = 1\ \mu M$. $[O_2]^{gas} = 1$ mM corresponds to 0.33 psi partial pressure of oxygen.

oscillations could be deactivation of HRP and Umb during the reaction. To check this a simulation assuming that there is no deactivation of HRP ($k_{13} = 0$) and Umb ($k_{17} = 0$) was performed. The results showed statistically insignificant decrease in standard deviation for oscillation period. Therefore, it was concluded that the change in the period is an attribute of the oscillation pattern and can be accounted for only by the complexity of the kinetic system. It should be noted that period of oscillations is the same for all oscillating species (see Fig. 3).

Fig. 5 shows how $[O_2]^{gas}$, $[O_2]_0^{aq}$, [IAA] and $[HRP]_0$ influence the period of oscillations. The plot of the period of oscillations vs. $[O_2]^{gas}$ has a minimum at $[O_2]^{gas} \approx 50$ mM (Fig. 5A), which corresponds to approximately the average of lower and upper values limiting the range of $[O_2]^{gas}$ in which the oscillations exist. Oscillations do not occur at 85 mM $< [O_2]^{gas} <$ 10 mM (see also Fig. 4). For further investigation $[O_2]^{gas}$ has been set at 43 mM which corresponds to 1 atm (14.2 psi) partial pressure of oxygen in the gaseous phase.

The period does not depend on the initial $[O_2]^{aq}$ within the range 0–40 μM and depends linearly on $[O_2]_0^{aq}$ over 50 μM (Fig. 5B). The lack of dependence on $[O_2]_0^{aq}$ for $[O_2]_0^{aq} < [O_2]_{cr}^{aq}$ can be explained in the following way. The reaction of IAA oxidation does not start until $[O_2]^{aq}$ reaches a certain value which is equal for all $[O_2]_0^{aq}$ less than $[O_2]_{cr}^{aq}$. Therefore, starting conditions are similar for all $[O_2]_0^{aq} < [O_2]_{cr}^{aq}$. In contrast, when the reaction starts at $[O_2]_0^{aq} > [O_2]_{cr}^{aq}$ then starting conditions depend on $[O_2]_0^{aq}$, and the period of oscillations also depends on $[O_2]_0^{aq}$.

Since the reaction model has been developed for $[IAA] = 100\ \mu M$, this value has been chosen for all the simulations except for those where [IAA] was a variable. This concentration is relatively low so that IAA consumption is fast and IAA concentration cannot be considered as quasi-constant. Usually, oscillation experiments are conducted at quasi-constant concentration of the substrate [11]. Therefore, [IAA] was assumed to be constant in all the experiments to prevent the influence of change in [IAA] on the oscillation pattern.

The plot of the period of oscillations vs. [IAA] has hyperbolic-like shape (Fig. 5C). Oscillations do not exist at $[IAA] < 50\ \mu M$. The period decreases with increasing [IAA] because at higher [IAA] the reaction rate is higher. Therefore, the period of time required for $[O_2]$ depletion in the reaction mixture decreases, which, in turn, results in a decrease in the overall period of oscillations. The period of oscillations does not approach zero since at a certain value

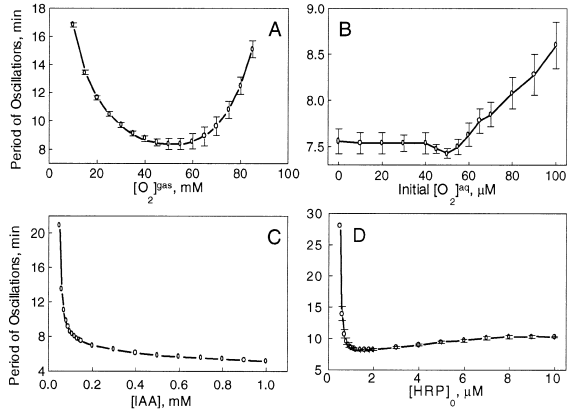

Fig. 5. The influence on the period of $[O_2]^{aq}$ oscillations of: (A) oxygen concentration in the gaseous phase, (B) initial oxygen concentration in the aqueous phase, (C) concentration of IAA and (D) initial concentration of HRP. The following parameters were used for the simulations: $k_{18} = 1 \times 10^{-6}\ s^{-1}$, $[O_2]_0^{aq} = 100\ \mu M$, $[O_2]^{gas} = 43$ mM (partial pressure 14.2 psi), $[HRP]_0 = 1\ \mu M$, $[IAA] = 100\ \mu M$ = constant and $[Umb]_0 = 1\ \mu M$ unless a parameter is a variable.

of [IAA] the rate-limiting factor for the reaction becomes the rate of oxygen intake (which does not depend on [IAA]) in the solution from the gaseous phase. This is confirmed by the fact that the period of oscillations decreases with increasing k_{18} (data not shown).

Fig. 5D shows the influence of $[HRP]_0$ on the period of oscillations. Oscillations do not exist at $[HRP] < 0.5$ μM. The period decreases rapidly with increasing $[HRP]_0$ until it reaches its minimum at $[HRP]_0 = 1.8$ μM. Further increase in $[HRP]_0$ results in only a slight increase in the period.

5.4. Amplitude of oscillations

Fig. 6 shows the influence of $[O_2]^{gas}$, $[O_2]_0^{aq}$, [IAA] and $[HRP]_0$ on the initial amplitude of oscillations. Initial amplitude increases with increasing $[O_2]^{gas}$ reaching the maximum at $[O_2]^{gas} = 70$ mM (Fig. 6A). Further increase of $[O_2]^{gas}$ results in decreasing the initial amplitude. Initial amplitude only slightly depends on $[O_2]_0^{aq}$ for 70 μM $< [O_2]_0^{aq}$ < 40 μM (Fig. 6B). There is a drop in the initial amplitude for 40 μM $< [O_2]_0^{aq} < 70$ μM. This obviously reflects the fact that the critical $[O_2]^{aq}$, around which the oscillations occur, is close to the value of 50 μM (Fig. 2). The amplitude decreases with increasing [IAA] (Fig. 6C). It could be explained neither by HRP deactivation to P-670 nor by Umb deactivation since assuming the rate constants of corresponding reactions, k_{13} and k_{17}, to be zero does not change considerably the way the initial amplitude depends on [IAA]. The dependence of the initial amplitude of oscillations on the initial HRP concentration has two extrema: the minimum at $[HRP]_0 =$ 1.8 μM and the maximum at $[HRP]_0 = 8$ μM (Fig. 6D).

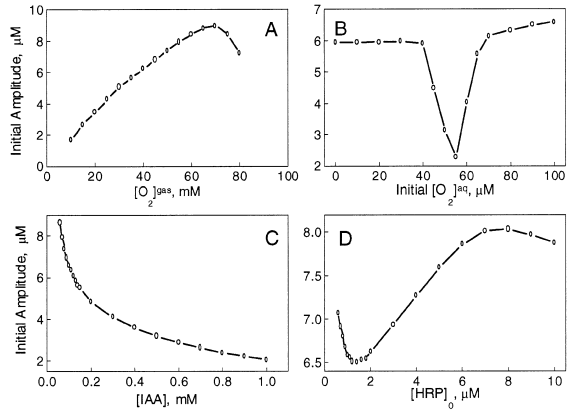

Fig. 6. The influence on the initial amplitude of $[O_2]^{aq}$ oscillations of: (A) oxygen concentration in the gaseous phase, (B) initial oxygen concentration in the aqueous phase, (C) concentration of IAA and (D) initial concentration of HRP. The following parameters were used for the simulations: $k_{18} = 1 \times 10^{-6}$ s^{-1}, $[O_2]_0^{aq} =$ 100 μM, $[O_2]^{gas} = 43$ mM (partial pressure 14.2 psi), $[HRP]_0 = 1$ μM, [IAA] = 100 μM = constant and $[Umb]_0 = 1$ μM unless a parameter is a variable.

It should be noted that the amplitude is not zero even though $[O_2]_0^{aq} = [O_2]_{cr}^{aq}$. This can be explained in the following way. As soon as the contact is established between the aqueous and gaseous phases oxygen starts to diffuse into the solution (if $[O_2]^{gas} > K_{eq}$ $[O_2]_{cr}^{aq}$). At this time there is no oxygen consumption because of a reaction lag period (see Section 5.1) [6,7]. Thus, when the reaction starts to consume oxygen, $[O_2]^{aq}$ already exceeds $[O_2]_{cr}^{aq}$ and oscillations occur.

Oscillations proceed around the steady state concentrations of the oscillating species. Steady state concentration which $[O_2]^{aq}$ approaches at infinite time was determined using Eq. (2) ($C^{max}(t_\infty)$ in the equation). It is found to be just a little higher than the critical oxygen concentration (Fig. 7).

Fig. 8 represents the influence of $[O_2]^{gas}$, $[O_2]_0^{aq}$, [IAA] and $[HRP]_0$ on the rate of damping of the oscillations. The rate of damping increases linearly with increasing $[O_2]^{gas}$ between 10 and 45 mM (Fig.

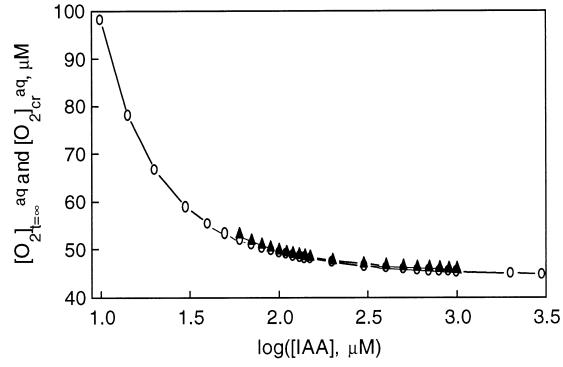

Fig. 7. Steady state concentration of O_2 at $t \to \infty$ (circles) and critical concentration of O_2 (triangles) in aqueous phase. Data for $[O_2]_{cr}^{aq}$ are taken from Fig. 2.

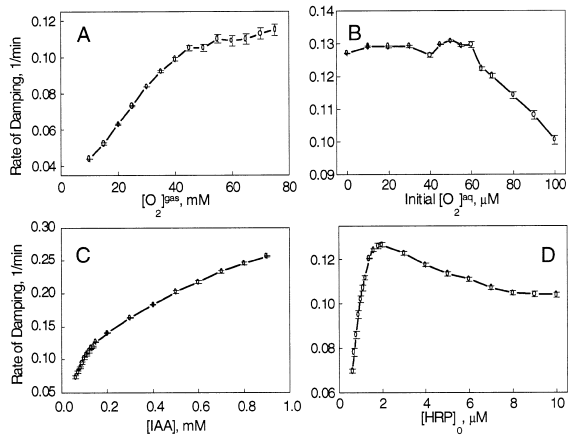

Fig. 8. The influence on the rate of damping for $[O_2]^{aq}$ oscillations of: (A) oxygen concentration in the gaseous phase, (B) initial oxygen concentration in the aqueous phase, (C) concentration of IAA and (D) initial concentration of HRP. The following parameters were used for the simulations: $k_{18} = 1 \times 10^{-6}$ s^{-1}, $[O_2]_0^{aq} = 100$ μM, $[O_2]^{gas} = 43$ mM (partial pressure 14.2 psi), $[HRP]_0 = 1$ μM, $[IAA] = 100$ μM = constant and $[Umb]_0 = 1$ μM unless a parameter is a variable.

8A). Further increase in $[O_2]^{gas}$ results in only a slight increase in the rate of damping. The rate of damping does not depend on $[O_2]_0^{aq}$ for $[O_2]_0^{aq} < [O_2]_{cr}^{aq}$ and decreases with increasing $[O_2]_0^{aq}$ for $[O_2]_0^{aq} > [O_2]_{cr}^{aq}$ (Fig. 8B). The rate of damping decreases gradually with increasing [IAA] (Fig. 8C). The plot of rate of damping vs. $[HRP]_0$ has maximum at $[HRP]_0 = 2$ μM (Fig. 8D).

5.5. The role of umbelliferone

Oscillations do not exist if the concentration of Umb is set to zero. Umb is a cofactor of HRP-catalyzed IAA oxidation with a complex mechanism of its influence on the reaction [9]. The presence of Umb results in acceleration of IAA oxidation due to three effects: (i) the reduction of HRP-II by Umb, (ii) oxidation of IAA by free radicals of Umb and (iii) Umb-induced acceleration of HRP-I reduction by IAA [9]. In spite of the complex mechanism of acceleration the role of Umb in appearance of oscillations is simply in its ability to increase the overall rate of IAA oxidation. Indeed, the effect similar to the presence of 1 μM Umb is simulated by 8-fold increase of k_{10} and k_{11} which results in 8-fold enhancement of the overall IAA oxidation, observed in the presence of 1 μM Umb [9]. Thus, the rate of IAA oxidation, rather than the presence of Umb itself, is critical for the occurrence of the oscillations. It is known that at lower pH the HRP-catalyzed oxidation of IAA is faster. Therefore, at lower pH oscillations can occur without a cofactor [16,17].

6. Concluding remarks

In conclusion, it should be noted that we deliberately did not reduce the system of 19 reaction steps resulting in 13 differential equations in this original study. It allowed us to trace all the features of damped oscillations in the complete system. Although the system of 13 differential equations is acceptable for a numerical study, it is too complicated for an analytical investigation. Such a system is certainly not the minimal system to account for damped oscillation. Therefore, further work on the IAA/HRP/O_2 oscillator may involve searching for a smaller system which would be compact enough to be handled analytically and detailed enough to describe a set of essential dynamic behaviors. Such a minimal system can be produced by sequential reduction of the system, using a number of judicious steady state assumptions.

It is also important to emphasize that the mechanism of IAA/HRP/O_2 oscillator described in this paper is rather different from that commonly accepted for the NADH/HRP/O_2 oscillator. In NADH-containing systems HRP-III plays a key role in the occurrence of the oscillations. In essence the oscillations in the NADH/HRP/O_2 system occur due to periodic transformations between active forms of the enzyme (HRP, HRP-I and HRP-II) and the relatively non-reactive HRP-III. In contrast, IAA/HRP/O_2 system does not involve HRP-III at neutral pH [5–9]. Periodicity in the IAA/HRP/O_2 system occurs exclusively due to interaction between consumption and accumulation of oxygen and reaction intermediates. The mechanism of IAA oxidation at low pH is probably very different from that at neutral pH [8]. It is known that HRP-III and consequently superoxide radical are involved in the reaction at acidic pH. Therefore, the mechanism and

patterns of oscillations in the IAA/HRP/O_2 system could be different at acidic and neutral pH. On the other hand, the mechanisms and patterns of oscillations in IAA/HRP/O_2 system at acidic pH could be similar to those for NADH/HRP/O_2 system. Further experimental studies will clarify these aspects.

Acknowledgements

The author is grateful to Dr. Leah Marquez for reading the manuscript and helpful comments.

References

[1] R. Nakajima, I. Yamazaki, J. Biol. Chem. 254 (1979) 872.
[2] A.M. Smith, W.L. Morrison, P.J. Milham, Biochemistry 21 (1982) 4414.
[3] J. Ricard, D. Job, Eur. J. Biochem. 44 (1974) 359.
[4] D. Metodiewa, M.P. de Melo, J.A. Escobar, G. Cilento, H.B. Dunford, Arch. Biochem. Biophys. 296 (1992) 27.
[5] S.N. Krylov, H.B. Dunford, Biophys. Chem. 58 (1996) 325.
[6] S.N. Krylov, H.B. Dunford, J. Phys. Chem. 100 (1996) 913.
[7] S.N. Krylov, H.B. Dunford, Photochem. Photobiol. 63 (1996) 735.
[8] S.N. Krylov, H.B. Dunford, in: C. Obinger, U. Burner, R. Ebermann, C. Penel, H. Greppin (Eds.), Plant Peroxidases: Biochemistry and Physiology IV, International Symposium, University of Geneva, 1996, p. 59.
[9] S.N. Krylov, H.B. Dunford, J. Phys. Chem. 100 (1996) 19719.
[10] D.L. Olson, A. Scheeline, J. Phys. Chem. 99 (1995) 1204.
[11] D.L. Olson, E.P. Williksen, A. Scheeline, J. Am. Chem. Soc. 117 (1995) 2.
[12] T. Odajima, I. Yamazaki, Biochim. Biophys. Acta 206 (1970) 71.
[13] G. Cilento, W. Adam, Photochem. Photobiol. 48 (1988) 361.
[14] I. Yamazaki, K. Yokota, R. Nakajima, Biochem. Biophys. Res. Commun. 21 (1965) 582.
[15] A. Scheeline, D.L. Olson, R. Larter, Chem. Rev. 97 (1997) 739.
[16] H. Degn, Biochim. Biophys. Acta 180 (1969) 271.
[17] H. Degn, D. Mayer, Biophys. Acta 180 (1969) 291.
[18] V.R. Fed'kina, F.I. Ataullakhanov, T.V. Bronnikova, Theor. Exp. Chem. 24 (1988) 165.
[19] S.N. Krylov, B.D. Aguda, M.L. Ljubimova, Biophys. Chem. 55 (1995) 213.
[20] S.N. Krylov, V.V. Lazarev, L.B. Rubin, Doklady Biophys. 310 (1990) 28.
[21] M.P. de Melo, T.C. Curi, R. Curi, P. Di Mascio, G. Cilento, Photochem. Photobiol. 65 (1997) 338.
[22] S.N. Krylov, A.B. Chebotareva, FEBS Lett. 324 (1993) 6.
[23] P.J. Davies, in: P.J. Davies (Ed.), Plant Hormones: Physiology, Biochemistry and Molecular Biology, Kluwer Academic, Dordrecht, 1995, p. 4.
[24] R.S. Bandurski, J.D. Cohen, J. Slovin, D.M. Reinecke, in: P.J. Davies (Ed.), Plant Hormones: Physiology, Biochemistry and Molecular Biology, Kluwer Academic, Dordrecht, 1995, p. 39.
[25] R.E. Cleland, in: P.J. Davies (Ed.), Plant Hormones: Physiology, Biochemistry and Molecular Biology, Kluwer Academic, Dordrecht, 1995, p. 214.
[26] S. Kobayashi, K. Sugioka, H. Nakano, M. Nakano, S. Tero-Kubota, Biochemistry 23 (1984) 4589.
[27] R. Nakajima, I. Yamazaki, J. Biol. Chem. 255 (1980) 2067.
[28] M. Acosta, M.B. Arnao, J.A. Del Rio, F. Garcia-Canovas, Biochim. Biophys. Acta 996 (1989) 7.
[29] I.G. Gazaryan, L.M. Lagrimini, G.A. Ashby, N.F. Thorneley, Biochem. J. 313 (1996) 841.
[30] V.V. Polevoi, Phytohormones, St. Petersburg Univ. Publishing, St. Petersburg, 1982, in Russian.
[31] W.H. Press, B.P. Flannery, S.A. Tenkolsky, W.T. Vetterling, Numerical Recipes: The Art of Scientific Computing, Cambridge Univ. Press, Cambridge, 1992.
[32] L.P. Candeias, L.K. Folkes, M.F. Dennis, K.B. Patel, S.A. Everett, M.R.L. Stratford, P. Wardman, J. Phys. Chem. 98 (1994) 10131.
[33] L.P. Candeias, L.K. Folkes, M. Porssa, J. Parrick, P. Wardman, Biochemistry 35 (1996) 102.
[34] T. Segawa, S. Suehara, T. Kamidate, H. Watanabe, Bull. Chem. Jpn. 67 (1994) 1301.
[35] S.N. Krylov, S.M. Krylova, I.G. Chebotarev, A.B. Chebotareva, Phytochemistry 36 (1994) 263.
[36] A. Lotka, J. Phys. Chem. 14 (1910) 271.